Journal of Industrial Microbiology, 3 (1988) 89–103
Elsevier



SIM 00119

# Investigation of differences in the tertiary structures of food proteins by small-angle X-ray scattering

Helmut Pessen, Thomas F. Kumosinski and Harold M. Farrell, Jr.

*Eastern Regional Research Center*, U.S. Department of Agriculture, Philadelphia, PA, U.S.A.*

Received 14 September 1987
Revised 17 December 1987
Accepted 21 December 1987

*Key words:* Food protein; Milk protein; Egg protein; Protein structure, tertiary; Small-angle scattering; β-Lactoglobulin; α-Lactalbumin; Lysozyme; Ribonuclease; Riboflavin-binding protein

## SUMMARY

With current emphasis in bioengineering on developing new and better structure-function relationships for proteins (e.g., the need for predictability of expected properties prior to cloning), practical and reliable methodology for providing characterization of appropriate features has become of increasing importance. The most potent and detailed technique, X-ray crystallography, has severe limitations: it is so demanding and time-consuming that X-ray coordinates are frequently unavailable for materials of interest; its data relate to static and essentially unhydrated structures, whereas proteins exhibit a variety of dynamic features and function in an aqueous environment; and many proteins of technological importance may never be crystallized. Small-angle X-ray scattering, however, is particularly suitable as a methodology that can provide a substantial number of significant geometric parameters consistent with crystallographic results, that can readily show tertiary structural changes occurring under varying conditions, and that can deal with solutions and gels. Results are presented here from small-angle X-ray scattering investigations of the apo and holo forms of chicken egg-white riboflavin-binding protein, chicken egg-white lysozyme, bovine milk-whey α-lactalbumin and β-lactoglobulin, and bovine ribonuclease. We utilize these observations to compare tertiary structures of these proteins as well as conformational changes in these structures, and to provide a basis for discussion of their physical and biological significance.

## INTRODUCTION

Biochemists and molecular biologists have invested much effort in studying the natural variations among specific protein molecules within a given family (e.g., point mutations and deletions), as well as in examining broader evolutionary changes which occur across species. Such comparisons have

* Agricultural Research Service, U.S. Department of Agriculture. Reference to brand or firm name does not constitute endorsement by the U.S. Department of Agriculture over others of a similar nature not mentioned.

Correspondence: H. Pessen, Eastern Regional Research Center, U.S. Department of Agriculture, Philadelphia, PA 19118, U.S.A.

brought about a clearer understanding of the structure-function relationships in proteins. With the advent of the new age of biotechnology, a myriad of new site-selected variants of enzymes and proteins have become possible, and the problem of rapid comparisons of these new substances has come to the fore. For genetically engineered enzymes, selection of the most appropriate form can be made on the basis of such criteria as substrate specificity or increased turnover number, but it must be borne in mind that any engineered change may in turn induce unforeseen changes in tertiary or quaternary structure leading to undesired alterations in physical properties, e.g., reduced solubility, or aggregations capable of blocking an active site. In the case of engineered food proteins, rapid methods for directly screening alterations in tertiary or quaternary structure seem warranted. In our laboratory small-angle X-ray scattering (SAXS) has been employed to study such structural changes.

SAXS is particularly suitable because, among the methods available for the characterization and study of globular proteins, it is one of the most powerful as well as versatile. When it is used on the absolute-intensity scale (i.e., when both the incident and the scattered intensities are quantified), this method is capable of yielding a variety of molecular parameters, such as the radius of gyration, maximum diameter, molecular weight, hydrated volume, surface-to-volume ratio, electron density, and degree of hydration of a particle in solution [4,26,37,64,65]. In addition, one may obtain the thermodynamic parameters of interacting systems [64], such as association constants of aggregating subunit systems and the degree of preferential interaction of proteins with components of mixed solvent systems.

In comparison with the ultimate method in structure determination, crystallography by X-ray or neutron diffraction, SAXS has both shortcomings and advantages. It is not capable of determining the coordinates of individual atoms in a molecular structure, as is crystallography. Such coordinates, however, are presently unavailable for many materials of interest and are not readily obtained except by a considerable investment in equipment and time. Moreover, X-ray diffraction is performed on samples in the crystalline state, i.e., on static structures, whereas proteins exhibit a variety of dynamic features increasingly recognized as crucial to their biological functioning; furthermore, notwithstanding the fact that they contain water of hydration, crystals are removed from the kind of aqueous environment in which proteins function and in which they may exhibit a variety of distinctive hydrodynamic features. SAXS, on the other hand, while giving results consistent with those of X-ray crystallography where available, is applicable to materials containing any desired amount of water, from dilute solutions to aggregates and gels.

The focus of this work is on the use of SAXS to show changes in tertiary structure which occur when proteins are subjected to altered environmental conditions; such changes can be used to monitor these conditions or to shed light on mechanisms or function. Presented here are the results of SAXS measurements which allow comparisons of related but significantly different structures of biological interest, such as the hen's egg-white enzyme lysozyme and the bovine milk-whey protein α-lactalbumin (α-La), thought to be evolutionarily related; and between both of these and an enzyme of similar size, bovine pancreatic ribonuclease. The relationships between the SAXS data and the published low-resolution diffraction data for the bovine milk-whey protein β-lactoglobulin (β-Lg) are examined for two natural genetic variants. Finally, in a case where no crystallographic structural data are available, changes are studied between the tertiary structures of the holo and apo forms of chicken egg-white riboflavin-binding protein (RBP) in reponse to pH variation, and in relation to the biological function of these changes.

## MATERIALS AND METHODS

### *Materials*

The β-Lg B and α-La were prepared from the unpasteurized milk of homozygous B/B cows and from pooled milk, respectively, according to the procedures described in Ref. 1. Chicken egg-white

lysozyme was the three-times-crystallized material of Pentex, Inc., Kankakee, IL. Bovine pancreatic ribonuclease was the salt-free five-times-crystallized product of Mann Research Laboratories, Inc., Orangeburg, NY. Homogeneities of these proteins were validated by sedimentation velocity, which in each case showed a single Gaussian peak. RBP was prepared by the method of Farrell et al. [18] and analyzed for purity electrophoretically on SDS gels by the method of Laemmli [34] with the use of 10% acrylamide. This method was used also to estimate the molecular weight of RBP, with the use of bovine serum albumin, ovalbumin, $\beta$-Lg, and $\alpha$-La as standards at 68000, 45000, 19000 and 15000, respectively.

Measurements of $\beta$-Lg were carried out in 0.1 M acetate buffer at pH 5.7, as in the work of Witz et al. [74]; those on $\alpha$-La in 0.1 M NaCl at pH 7.0 and those on lysozyme in 0.15 M NaCl at pH 3.8, both following Krigbaum and Kügler [29]; those on ribonuclease in 0.1 M acetate buffer at pH 5.2; those on RBP at pH 3.7 in 0.005 M phosphate buffer containing 0.1 M NaCl for the apoprotein, and a pH 7.0 also in 0.005 M phosphate with 0.1 M NaCl for both apo- and holoprotein. All buffer chemicals were reagent grade.

Sample solutions were prepared by dissolving the particular protein in 4–6 ml of the appropriate solvent, adjusting the pH to the desired value, and dialyzing against three 1-liter changes of solvent. Required dilutions were made with the final dialyzate. Protein concentrations, ranging roughly from 10 to 80 mg/ml, depending on the protein, were determined spectrophotometrically with absorption coefficient values of 0.96 $l \cdot g^{-1} \cdot cm^{-1}$ for $\beta$-Lg at 278 nm [70], 2.01 for $\alpha$-La at 280 nm [31], 2.60 for lysozyme at 280 nm [27], 0.698 for ribonuclease at 277.5 nm [13], and $4.9 \times 10^4$ $M^{-1} \cdot cm^{-1}$ for apo-RBP at 282 nm [58], respectively, or also, in the case of the latter, by the method of Lowry et al. [35].

The values of the partial specific volume, $\bar{v}$, used were 0.751 ml/g for $\beta$-Lg [47], 0.729 for $\alpha$-La [23], 0.7138 for lysozyme [11], 0.7075 for ribonuclease [15,57], and 0.720 for RBP [52]. The number of electrons per gram, $q$, for each protein was calculated from its amino acid composition [22,8,10,59,18, respectively]. The resulting values of $q$ and the electron partial specific volume, $\psi = 10^{24}\ \bar{v}/q$, were $0.3221 \times 10^{24}$ $e^-/g$ and 2.332 $A^3/e^-$, respectively, for $\beta$-Lg, $0.3178 \times 10^{24}$ and 2.293 for $\alpha$-La, $0.3209 \times 10^{24}$ and 2.225 for ribonuclease, and $0.303 \times 10^{24}$ and 2.376 for RBP. The electron densities of the solvents were calculated as 0.355 $e^-/A^3$ for the case of RBP and 0.335 $e^-/A^3$ for all others.

*Apparatus*

The apparatus employed was an absolute-scale small-angle X-ray scattering instrument designed and constructed at this laboratory. It is a directly referenced, symmetrically scanning, vertical-axis instrument with sealed-window proportional detection, used in the continuous-scan mode with time constants of appropriate length. The $CuK_{\alpha 1}$ radiation from a fine-focus tube operated at 40 kV and 25 mA was selected by the curved quartz-crystal primary-beam monochromator. Full details of this instrument and operational procedures have been given earlier [50].

*Data evaluation*

The working equations and the notation used are essentially those of Luzzati et al. [38,39], with some modifications. They apply to globular particles in the case of so-called 'infinite slit' collimation (i.e., very high slit height-to-width ratio), conditions satisfied by the instrument and the systems under examination. The expression relating the excess scattered intensity for a slit source, $j_n(s)$, (scattered intensity of sample, normalized with respect to the intensity of the incident beam and corrected for scattering of blank) to the scattering angle $2\theta$ is [38]:

$$j_n(s) = j_n(0) \exp\left[-(4/3)\pi^2 R_a^2 s^2\right] + \varphi(s) \qquad (1)$$

where $s \equiv (2 \sin \theta)/\lambda$, $\lambda$ is the wavelength of the radiation used (1.540 Å), $j_n$ (0) is the normalized intensity extrapolated to zero angle, $R_a$ is the apparent radius of gyration (i.e., the root-mean-square distance of all the electrons in the solute particle from its center of electronic mass) obtained by slit collimation at a finite concentration of solute [36],

and $\varphi(s)$ is a function expressing the residual between the Gaussian part of Eqn. 1 and the scattering actually observed. For small values of $s$ (i.e., $s < 2.5 \times 10^{-2}$ Å$^{-1}$, or $2\theta < 2°$), $\varphi(s)$ is always negligible compared with the first term, which represents the Guinier approximation [25]. $R_a$ can therefore be obtained from the Gaussian fit to $j_n(s)$ vs. $s^2$ for the region of very small angles. Since, however, the theoretical point-source scattering function $i_n(s)$ was needed later in any event, it was constructed from the smeared infinite-slit data $j_n(s)$ by deconvolution [38], and the concentration-dependent point-source radius of gyration $R_i$ was, in fact, obtained in place of $R_a$ in an analogous manner.

After evaluating $i_n(0)$ by extrapolation of $i_n(s)$ to zero angle, it was possible to calculate

$$m_{app} = i_n(0)(1-\rho_1\psi_2)^{-2}c_e^{-1} \tag{2}$$

$$m = m_{app} + 2Bm^2c_e \tag{2a}$$

$$M = mN_A/q \tag{2b}$$

Here $m_{app}$ is the apparent molecular mass, expressed as electrons/molecule, at concentration $c_e$, $c_e$ is the concentration in electrons of solute/electron of solution, $m$ is the molecular mass obtained by extrapolation to zero concentration of a plot of $m_{app}$ vs. $c_e$, $\rho_1$ is the electron density of the solvent, and $\psi_2$ is the electron partial specific volume of the solute, defined in terms of $\bar{v}$ and $q$ under Materials and Methods above. $B$ is the second virial coefficient, $M$ is the weight-average molecular weight, and $N_A$ is Avogadro's number.

Introduction of a corrected normalized scattering intensity $j_n^*(s)$ defined by

$$j_n^*(s) = j_n(s) - \delta^* \tag{3}$$

where $\delta^*$ is a correction term reflecting short-range electron-density fluctuations due to the internal structure of the particle, leads to the equation

$$s^3j_n^*(s) = s^3j_n(s) - \delta^*s^3 \tag{3a}$$

illustrated by the Soulé-Porod plots [54,60] of $s^3j_n(s)$ vs. $s^3$ (cf. Figs. 1B and 3B). The straight line fitted to such a plot at intermediate and higher values of $s$, where the gradually diminishing oscillations of the curve permit a fairly reliable fit of a straight line as a mean, provides an asymptotic approximation represented by

$$\lim_{s\to\infty} s^3j_n(s) = \lim_{s\to\infty} s^3j_n^*(s) + \delta^*s^3 \tag{3b}$$

which allows the evaluation of the constants $\delta^*$ and $\lim_{s\to\infty} s^3j_n^*(s)$ (both needed for subsequent expressions) from the slope and intercept of the asymptote, respectively. (To be strictly consistent, $j_n^*(s)$ should have been used in place of $j_n(s)$ in Eqn. 1, but the value of $R_a$ is not actually affected by the correction of $\delta^*$ [38], in contrast to the equations that follow.)

With the use of these constants, further parameters were calculated [38]:

$$V = i_n(0)/\int_0^\infty 2\pi s j_n^*(s)\mathrm{d}s \tag{4}$$

$$S/V \simeq \frac{16\pi^2 \lim_{s\to\infty} s^3j_n^*(s)}{\int_0^\infty 2\pi j_n^*(s)\mathrm{d}s}\left[1 - \frac{c_e\rho_2(1-\rho_1\psi_2)}{\rho_2-\rho_1}\right] \tag{5}$$

$$\Delta\rho = \rho_2-\rho_1 \simeq \frac{\int_0^\infty 2\pi s j_n^*(s)\mathrm{d}s}{c_e(1-\rho_1\psi_2)} + c_e\rho_1(1-\rho_1\psi_2) \tag{6}$$

$$\mathrm{H} = \frac{\rho_1(1-\rho_2\psi_2)}{\Delta\rho} \tag{7}$$

Here $V$ is the hydrated volume, $S$ is the external surface area of the particle, $\rho_2$ is the mean electron density of the hydrated particle, in electrons/Å$^3$, $S/V$ is the surface-to-volume ratio, and $H$ is the degree of hydration in electrons of bound $H_2O$/electron of dry particle, from which the conventional degree of hydration, expressed as the number of grams of water of hydration per gram

of dry protein, can be obtained by a simple conversion. Tabulated parameters (such as the point-source radius of gyration $R_G$, derived from the concentration-dependent point-source radius of gyration $R_i$) were obtained by extrapolation to zero concentration.

Assuming as a model prolate ellipsoids of revolution, one can calculate from $R_g$ and $V$ axial ratios $p \equiv a/b$ (where $a$ is the semiaxis of revolution and $b$ the equatorial radius), making use of the relationship

$$3V/(4\pi R_G^3) = 5p^{2/3}/(2p^2)^{3/2} \quad (8)$$

from which $p$ could be obtained graphically [38]. We solved for $p$ by iteration, using a programmable desk calculator.

## RESULTS

The final results are summarized in Table 1. It may be noted that, as experience with instrument and technique became refined, the number of parameters and the precision of data increased.

*β-Lactoglobulin*

Data collected on a relative scale over an angular region from $-2$ to $+2°$ for solutions at concentrations from 12 to 61 mg/ml were treated according to Eqn. 1. The resulting Guinier plots (plots of the natural logarithm of the excess scattered intensity vs. the square of the scattering vector $s$) have slopes of $-(4/3)\pi^2 R_a^2$, from which values of $R_a$ were obtained. Plotted against the corresponding concentrations, $R_a$ showed no concentration dependence, so that the value listed was taken as the average.

*Lysozyme, α-La, and ribonuclease*

The data were collected on an absolute scale over an angular range of $-5$ to $+5°$ for concentrations from 10 to 50 mg/ml and evaluated according to Eqns. 1–8. Typical Guinier plots (Eqn. 1) and Soulé-Porod plots (Eqn. 3) are shown in Fig. 1A and B. Concentration plots are shown in Fig. 2. For lysozyme and α-La, none of the parameters exhibited a concentration dependence. By contrast, most of the parameters for ribonuclease were distinctly concentration-dependent and required extrapolation to zero concentration. The apparent

Table 1

SAXS parameters of five proteins[a]

| Parameter[b] | β-Lg | α-La | Lysozyme | Ribonuclease | Holo-RBP (pH 7.0) | Apo-RBP (pH 3.7) |
|---|---|---|---|---|---|---|
| $R_G$, Å | 20.8 ± 0.4 | 14.5 ± 0.2 | 14.3 ± 0.2 | 14.8 ± 0.4 | 19.8 ± 0.2 | 20.6 ± 0.1 |
| $M$ | | 14 200 ± 600 | 14 300 ± 300 | 13 700 ± 800 | 33 800 ± 400 | 35 000 ± 800 |
| $V$, Å$^3$ | | 25 100 ± 800 | 24 200 ± 400 | 22 000 ± 700 | 55 600 ± 530 | 66 500 ± 240 |
| $S/V$, Å$^{-1}$ | | 0.24 ± 0.02 | 0.25 ± 0.03 | 0.29 ± 0.02 | 0.213 ± 0.001 | 0.203 ± 0.001 |
| $\Delta\rho$, e$^-$/Å$^3$ | | 0.067 ± 0.002 | 0.078 ± 0.002 | 0.071 ± 0.002 | 0.0626 ± 0.0005 | 0.053 ± 0.0004 |
| $H$, g ($H_2O$)/g (dry protein) | | 0.36 ± 0.03 | 0.32 ± 0.02 | 0.27 ± 0.04 | 0.27 ± 0.01 | 0.38 ± 0.01 |
| $a/b$ | | 1.43 | 1.42 | 1.87 | 1.77 ± 0.05 | 1.63 ± 0.03 |
| $(a/b)_v$[c] | | | | | 3.62 ± 0.04 | 3.57 ± 0.05 |

[a] Error terms represent the standard error of the parameter.

[b] Definitions and procedures for obtaining these parameters are as given under Materials and Methods.

[c] See Discussion.

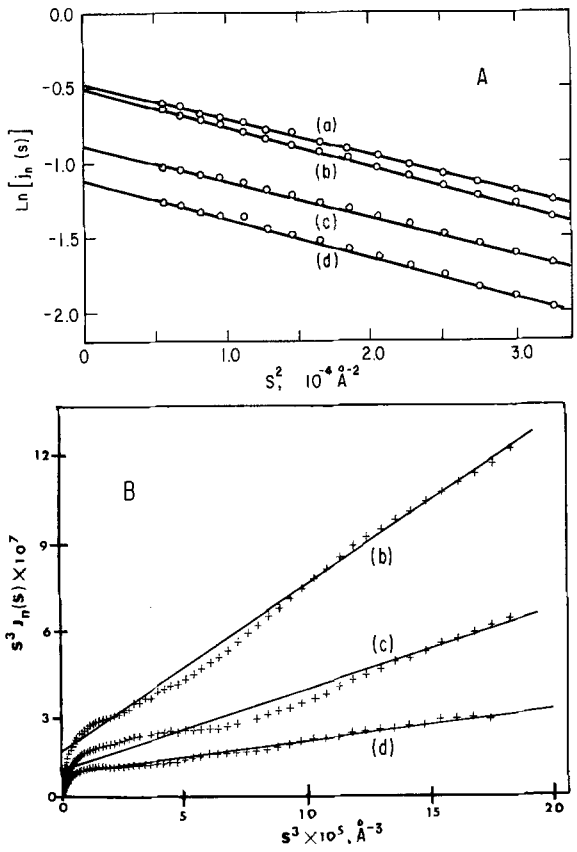


Fig. 1. Typical scattering functions from slit-smeared data for lysozyme at several concentrations: (a) 45.0 mg/ml; (b) 36.0 mg/ml; (c) 27.0 mg/ml; (d) 21.6 mg ml. (A) Semi-logarithmic plot of normalized slit-source scattered intensity vs. square of scattering angle (Guinier plot). (B) Plot of $s^3 j_n(s)$ vs. $s^3$ (Soulé-Porod plot).

radius of gyration and the molecular volume decreased slightly, the molecular weight and the hydration decreased considerably, and the apparent electron density difference increased with concentration, while the surface-to-volume ratio showed no concentration dependence.

*RBP apo and holo forms*

Absolute intensity measurements were made over an angular range from $-5$ to $+5°$, for protein concentrations from 15 to 80 mg/ml and were evaluated as before. Typical Guinier plots and Soulé-Porod plots are shown in Fig. 3A and B; concentration plots are shown in Fig. 4. For both the apo- and the holoprotein, the apparent radius of gyration was independent of concentration, as were the surface-to-volume ratio, the electron density difference, and the hydration for the holoprotein. The apparent molecular volume and molecular weight of the holoprotein decreased slightly with concentration, as did the molecular volume, molecular weight, electron density difference, and surface-to-volume ratio for the apoprotein; for the apoprotein also, the hydration increased slightly. These parameters, therefore, required extrapolation to zero concentration.

## DISCUSSION

*β-Lg B*

The value of the radius of gyration found, 20.8 ± 0.4 Å, compares with values of 21.7 ± 0.2 Å for β-Lg B and 21.6 ± 0.4 Å for β-Lg A reported by Witz et al. [74]. Green et al. [24], in a low-resolution X-ray diffraction study of β-Lg A and B determined parameters from which a radius of gyration of 21.8 Å was calculated [74].

This protein has been reported to occur in nature in at least seven genetic variants [14]. The most studied of these, the A and B variants, can undergo a variety of changes in conformation and state of association, summarized in part in Fig. 5. Among the most notable of these are a slow, irreversible high-pH denaturation [71] and a rapid dimer ⇄ octamer equilibrium [33,66–69], both occurring primarily in the cold. The 2-subunit 36700-dalton dimer is the kinetic unit persisting over a wide range of moderate conditions of pH from 3 to about 7 [66].

Apart from some less notable differences in physical properties, the differences between the variants in denaturation and association behavior are the most striking. At pH 6.5, the dimer is known to begin to dissociate [20,43,70], followed by a time-dependent denaturation [9,20,56]. This 'cold denaturation' occurs about three-times faster with β-Lg A than with B [71] and correlates with increased hydration under the same conditions found by Pessen et al. [51] in a nuclear magnetic resonance (NMR) study of these variants.

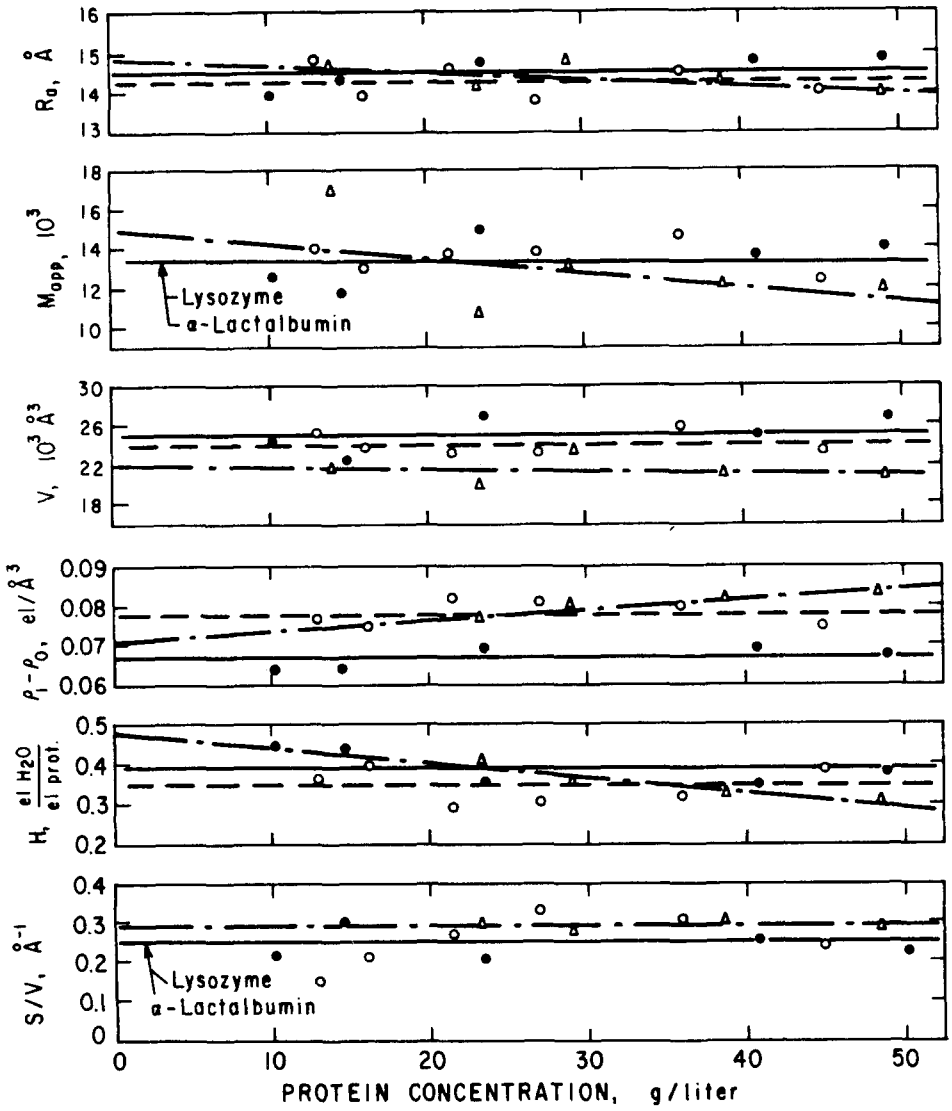


Fig. 2. Concentration dependence of six computed molecular parameters (radius of gyration, molecular weight, hydrated volume, electron density difference, degree of hydration, surface-to-volume ratio) for lysozyme (---○---), α-La (-●-), and ribonuclease (-·△·-).

Between pH 3.7 and 5.1, self-association of dimer to octamer takes place as temperature decreases. This rapid-equilibrium process has also been well characterized [33]. It occurs to a markedly greater extent with the A variant than with the others; e.g., at 2°C and pH 4.65, the optimum, octamer formation is over 90% complete for β-Lg A vs. 31% for β-Lg B, as calculated from the light-scattering data of Kumosinski and Timasheff [33]. This process also correlates exceedingly well with increased hydration [51].

The basic difference between the variants is in the primary structure, where B differs from A by two substitutions in the 162-amino acid sequence, namely a Gly in B for an Asp in A in position 64, and an Ala for a Val in position 118. Although this must be the direct (or indirect) cause of the differences in behavior described above, it evidently is not sufficient to result in a difference in the radius of gyration at room temperature, where our scattering work was carried out.

An interesting recent observation is that β-Lg

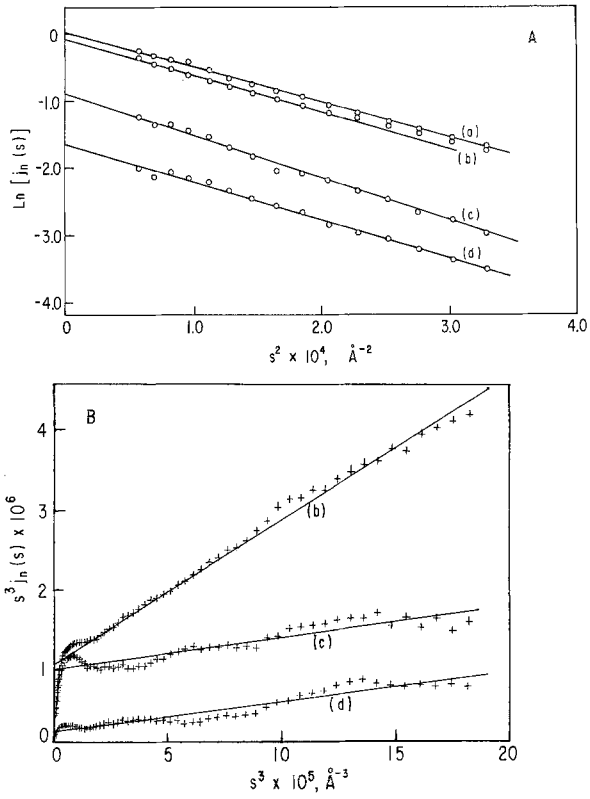


Fig. 3. Typical scattering functions from slit-smeared data for apo-RBP at pH 3.7 at several concentrations: (a) 70.9 mg/ml; (b) 62.9 mg/ml; (c) 21.0 mg/ml; (d) 12.6 mg/ml. (A) Semi-logarithmic plot of normalized slit-source scattered intensity vs. square of scattering angle (Guinier plot). (B) Plot of $s^3 j_n(s)$ vs. $s^3$ (Soulé-Porod plot).

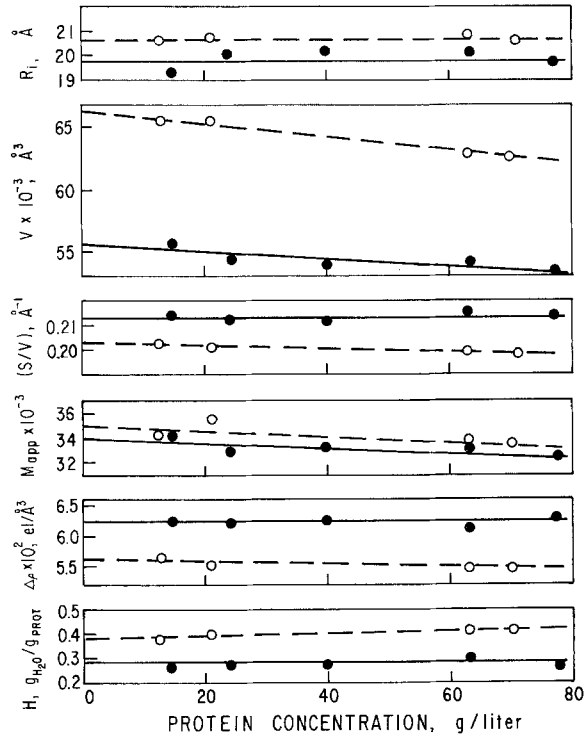


Fig. 4. Concentration dependence of six computed molecular parameters (radius of gyration, hydrated volume, surface-to-volume ratio, molecular weight, electron density difference, degree of hydration) for RBP holoprotein (-●-) and apoprotein (--○--).

has a strong structural homology with serum retinol-binding protein [21,49]; in fact β-Lg binds retinol as well as other aromatic compounds [16]. The point mutations discussed above have been found to influence binding of aromatics to a marked extent. Thus, the association constants for complex formation with *p*-nitrophenyl phosphate by the genetic variants β-Lg A, B and C are, respectively, 32, 16 and 14 × $10^3$ $M^{-1}$ [16]. The pH dependence of the β-Lg molecular structure, however, may also relate to binding, and this has not been tested. In the light of our own findings on RBP below it may be of interest to examine structural changes occurring below pH 3.5, where β-Lg becomes monomeric and aromatics are released.

*Lysozyme and α-La*

No statistically significant difference between these two proteins is found for the values of molecular weight and surface-to-volume ratio, and only a very slight, probably not significant difference for the radii of gyration and the molecular volumes. Values for the electron density difference and the degree of hydration differ more significantly. The axial ratios of the scattering-equivalent ellipsoids of revolution are virtually indistinguishable.

These findings are in essential agreement with the expectations raised by the homologous amino acid sequence portions of the two proteins and the consequent conjecture of conformational similarity. The sequence homologies are very substantial, extending to better than 30% of the chain and including the position of the four disulfide bridges [8]. Furthermore, the replacements of amino acid residues necessary to change the sequence of lysozyme

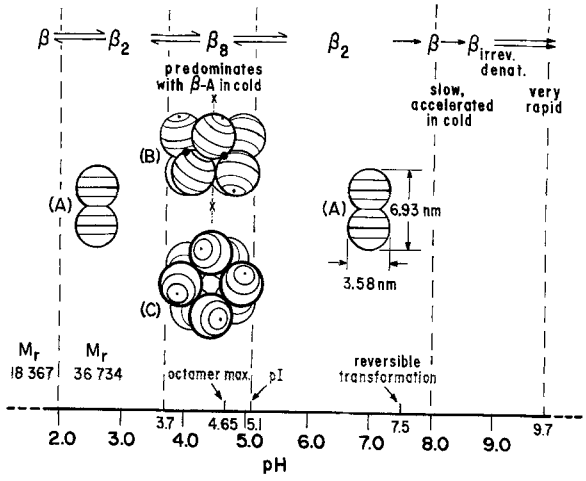


Fig. 5. Schematic representation of changes in the structure of β-lactoglobulins as a function of pH. β:β-La. Insets (molecular models): (A) dimer; (B) octamer, with square decahedral faces on top and bottom; O, octamer bonds; x-x, tetrad axis; circular lines indicate monomer equators and parallels perpendicular to the dimer axes; (C) octamer, with square faces in front and back, tetrad axis perpendicular to plane of paper. (Based on Refs. 9, 20, 24, 33, 43, 51, 56, 63, 66–69, 71.)

to that of α-La are functionally conservative, in that they can be accommodated by the same secondary and tertiary structure [72]. Extensive investigations using optical rotatory dispersion, circular dichroism, infrared and NMR spectroscopy [2,12,30] observed only small differences which could be fully accounted for on the basis of dissimilar side chains. An immunological study [61] detected a weak cross-reaction; immunological findings, however, resulting presumably from similar residues in exposed parts of the two proteins, cannot be conclusive regarding molecular conformation because of their limited significance with respect to the portions of the chain responsible for maintaining the three-dimensional structure.

X-ray scattering, which gives more direct knowledge of conformation, furnishing at the same time independent information on molecular size and shape, would be more pertinent. An earlier SAXS investigation [29] appeared to have found some substantial differences between lysozyme and α-La. In our work we have not been able to reproduce these differences. Thus we conclude that, except for a small difference in the extent of hydration, the two proteins have closely similar macromolecular parameters. This result confirms the report of Warme et al. [72] that the amino acid sequences of both proteins can be accommodated by the same three-dimensional folding of the polypeptide chains.

It may be, however, that the diversity in these results, while real, is reconcilable. It has recently been shown that α-La is actually a calcium-binding protein [32,48]. With this information, elucidation of the X-ray crystallographic structure of holo-α-La, and in particular its $Ca^{2+}$-binding site, has now progressed rapidly [62]. Murakami et al. [44] have shown enhanced structural stability in α-La owing to the presence of $Ca^{2+}$. In our experience the degree of calcium bound to the protein is highly dependent upon the method of preparation. The differences in SAXS data between laboratories, therefore, might well be due to small changes in conformation or stability occurring upon binding of $Ca^{2+}$. Thus a reinvestigation of holo- and apo-α-La under controlled conditions might reveal discrepancies in such changes as a result of varying degrees of metal-ion binding.

*Ribonuclease*

In view of the similarity of results obtained for lysozyme and α-La, it could be suggested that X-ray scattering as a method might not be sensitive enough to distinguish between two globular proteins of very similar size. In this connection the results for ribonuclease, another globular protein of also approximately the same size (see Table 1), are of interest. Of the parameters for this protein, the molecular weight shows no statistically significant difference compared to either lysozyme or α-La, but the radius of gyration is somewhat higher compared to either, the surface-to-volume ratio and the axial ratio are significantly higher, and the molecular volume and the hydration are significantly lower. The electron density difference for ribonuclease is the only parameter intermediate between those of the other two proteins and is again distinctly different from each. Also of interest is a distinct concentration dependence of nearly all these parameters (except only the surface-to-volume ratio) in

the case of ribonuclease, whereas in general no significant dependence was observed for lysozyme or α-La.

Compared with lysozyme and α-La as a group, ribonuclease thus presents a distinctly different picture. It is apparent that while no very substantial size or shape differences were observed between lysozyme and α-La, significant differences may be seen between either of these proteins on the one hand and ribonuclease on the other. More extensive differences permitting more detailed conclusions would probably be detected on extending the studies to higher scattering angles (and, because of the diminished scattering, necessarily to higher concentrations), where intraparticle interference effects would be more notable and the shape factor would become of greater consequence.

*RBP*

RBP occurs in the yolks and whites of all avian eggs [46]. It is responsible for the transport of riboflavin through the blood stream of the laying hen and into the eggs, where the vitamin is essential for embryonic growth and development [17,19]. The absence of this protein from the blood and eggs of a mutant strain of chickens leads to the death of the developing embryo by reason of a gross riboflavin deficiency [42,73]. Studies of the reversible binding of riboflavin to RBP have yielded values for the association constant of $10^9$–$10^{10}$ $M^{-1}$ [3,45]. This strong binding serves the function of transport well: it appears that the vitamin is released to the embryo at low pH, since the pH profile for binding of riboflavin to the protein shows that below pH 4.0 the binding drops off rapidly, with an apparent p$K$ at 3.8 [7,18]. This release could be due to protonation of specific residues, or to more generalized phenomena relating to changes in the structure of the protein.

Neither the amino acid sequence nor the X-ray crystallographic structure of RBP is known. In the absence of such basic structural information, SAXS parameters relating to the protein both above and below the p$K$ of binding can be used for correlating observed structural changes with the binding and release of riboflavin by RBP.

Comparison between the SAXS parameters in Table 1 for the two forms of the protein at pH 7.0 and pH 3.7 shows that, in going from the holo to the apo form, the radius of gyration increases from 19.8 to 20.6 Å. The difference of 0.82 (with a standard deviation of the difference of the means of 0.19 Å) is relatively small but statistically significant. It is of the same order of magnitude, and in the same direction, as comparable changes in radius of gyration found by other workers from SAXS in cases where proteins bind ligands of roughly similar size. For yeast hexokinase, Steitz and co-workers [40,41] found that on binding glucose there was a reduction in radius of gyration of 0.95 ± 0.24 Å; on binding glucose 6-phosphate the reduction was 1.25 ± 0.28 Å. On binding 3-phosphoglycerate to phosphoglycerate kinase there was a 1.09 ± 0.34 Å reduction [53]. Quiocho et al. [55], studying similar changes in a number of sugar-binding proteins, determined a decrease of 0.94 ± 0.33 Å in radius of gyration upon binding of arabinose to L-arabinose-binding protein. In these instances, the X-ray crystallographic structures were known, and radii of gyration computed from them were in close agreement with those found from SAXS. Crystallographic data further showed a clear conformational difference between apo and holo forms of the protein and indicated that the mechanism of binding depended on an allosterically induced closure of a cleft in the molecule. Except for the radius of gyration, no other structural SAXS parameters were used in the study of these systems; in fact, in no case were any SAXS parameters, such as $V$, $S/V$, $a/b$ or $H$, reported.

Several of the parameters listed in the table undergo changes which are significant and warrant discussion. The marked increase in volume accompanying release of the riboflavin at low pH must be indicative of swelling, due to increased hydration, structural changes, or both. The increase in $H$ from 0.27 to 0.38 g $H_2O$/g dry protein shows that hydration certainly is a factor; it corresponds to a presumptive increase from about 500 to 700 molecules of water/protein molecule. But even allowing a volume of 30 $Å^3$ per molecule of water (estimated from the specific volume of bulk water), the difference of

about 200 molecules could account for at most about 7000 Å$^3$ of the 10900 Å$^3$ increase in hydrated volume seen from Table 1. A considerable amount of structural swelling must, therefore, occur, perhaps owing to the reversal of net charge, since the protein at pH 3.7 is below its isoelectric point.

Inspection of the relative changes in some of the parameters (+4% for $R_G$, +20% for $V$, −5% for $S/V$) discloses that they are roughly consistent with one another from simple dimensional considerations, although the change in $R_G$ is slightly less than would be expected from the corresponding changes in $V$ and $S/V$. This is a hint of some decrease in anisotropy. A combined consideration of the parameters leads to some further information. Since the expression $3V/(4\,\pi\,R_G^3)$ is dimensionless, it must be characteristic of a family of spheroids of equal anisotropy and must be a function of the axial ratio $a/b$ only [38]. Conversely, $a/b$ can be calculated from the dimensionless ratio (by straight-forward numerical methods, if not in closed form). The values listed in Table 1 show that there is indeed a small but significant decrease from 1.77 to 1.63; i.e., the molecule at pH 3.7 has become somewhat more rounded as well as bulkier. If the molecule is assumed to be a prolate ellipsoid of revolution one may, from the values of $a/b$ and $V$, obtain the values of the respective half-axes ($a$ = 34.6 ± 0.6, $b$ = 19.6 ± 0.2 Å, for the holoprotein; $a$ = 34.8 ± 0.5, $b$ = 21.4 ± 0.2 Å, for the apoprotein). The differences between the parameters of holo- and apo-RBP in every one of the preceding instances, as well as in nearly all of those to follow, are statistically significant (by $t$-test, $P < 0.01$, in all cases except for $\Delta\rho$ and $(a/b)_v$, where $P \simeq 0.1$, and $a$, where $P > 0.2$). The difference in $a$ is thus not significant at any reasonable probability level. It may, therefore, be concluded that both the decrease in anisotropy and the increase in volume are due mainly to an enlargement of the minor axis.

By methods analogous to those used to obtain $a/b$, a value for a virtual axial ratio $(a/b)_v$ may be obtained from a second dimensionless ratio used by Luzzati et al. [38], $R_G\,S/V$. This, in contrast to the first, includes a parameter that is a measure of surface. The resulting $(a/b)_v$ (holo-RBP, 3.62; apo-RBP, 3.57) clearly does not represent a 'real' ellipsoid but some scattering-equivalent ellipsoid of identical volume. This second model attempts to compensate in terms of the smooth surface of a hypothetical, elongated body for the textured surface of the more compact actual body, which would not be amenable to characterization by two simple parameters ($a$ and $b$). (These parameters, since they are based on three independent equations (one for each of the experimental quantities $R_G$, $S$, and $V$), are algebraically overdetermined and will not yield a calculated value for $R_G$ identical to the experimental one. Nonetheless, since it does take into account surface features, this is a useful alternative model to employ for comparisons with the surface-sensitive data obtained from hydrodynamic phenomena).

To examine the data relating to surface area more closely, it will be convenient to distinguish between several separate contributions to the total surface as follows. (1) There is the surface of the basic model, i.e., the ellipsoid of revolution having the volume and radius of gyration found by SAXS independently of any model assumptions. Its surface area, as a first approximation to that of the molecule, may be designated as $S_M$, the model surface. (2) It is recognized that the assumption of an ellipsoid of revolution is arbitrary and is made only as a point of departure because of its mathematical convenience. The real model is certain to vary from this idealization and to be less readily characterizable. A closer approximation might utilize some other shape, such as a more general ellipsoid with three different axes, a cylinder or conical frustum with rounded edges, or a kidney. Without attempting to go into details of such geometries, we may assume that for any such body with identical volume and radius of gyration the corresponding surface area will be somewhat larger than $S_M$. To take the difference into account, we consider it as an excess surface, $S_B$, the additional contribution to surface due to deviation in overall body shape from the spheroidal model. (3) It is obvious that the surface of a molecule which consists of coiled, folded, and unordered chains, as does a protein, cannot be smooth. Superimposed on the body shape will be

such textural features as wrinkles, small protuberances, clefts, or localized grooves. These will make a substantial contribution to surface which we designate as $S_X$, the additional contribution to surface due to texture. When convenient, $S_B$ and $S_X$ might be lumped together as $S_T$, the excess topographical surface. If we assign all conceivable contributions to total surface to one of the foregoing three categories, $S_M$, $S_B$, or $S_X$, then $S_M + S_B + S_X$ must equal $S_{tot}$, the total surface area.

As a measure of $S_{tot}$ we take the surface $S$ found from experiment. Using the respective values for $V$ and $S/V$ from Table 1, we have $S_{tot}$ equal to 11 840 $\pm$ 120 Å$^2$ for holo-RBP and 13 470 $\pm$ 140 Å$^2$ for apo-RBP. For $S_M$, using the appropriate geometric expression for elliptical surface in terms of $a$ and $b$, we calculate 7420 $\pm$ 30 Å$^2$ and 8250 $\pm$ 30 Å$^2$, respectively. It is noteworthy that the ratio $S_M/S_{tot}$ is 0.63 $\pm$ 0.01 and 0.61 $\pm$ 0.01, respectively. It follows that $S_T/S_{tot}$, the remaining fraction of about 0.38, also is the same, or nearly so, for both forms of the protein; i.e., the increased $S_{tot}$ remains divided in nearly the same proportions between $S_M$ and $S_T$. Even without specific knowledge of $S_B$ (obtainable, for example, from a more detailed shape analysis not undertaken here), there is some pertinent information available because the shape of a scattering particle gives rise to very characteristic fluctuations in the various scattering curves, as discussed, e.g., by Kratky [28] and as seen in the Soulé-Porod plots of Fig. 3B. Shapes and positions of the minima and maxima in this figure did not change between apoprotein and holoprotein (the latter not shown here), and similar minima and maxima in the tails of the primary scattering curves (e.g., $j_n(s)$ vs. $s$), where they show up even more sharply, remained equally undisplaced. Whatever $S_B$ might be, it thus cannot differ by much between the two forms of RBP in the absence of a change in body type or any major change in shape within the same body type. From a consideration of the behavior of $S_{tot}$, $S_N/S_{tot}$, and $S_B$, it may be concluded that at low pH not only does $S_X$ increase in absolute terms, but as a fraction of total surface it must also increase to some extent depending on $S_B$. That is, the new textural surface must be, at minimum, in proportion to the new total surface. In looking for a structural change to fit this geometry, one finds that it can be accounted for by a cleft which opens to supply this increased textured surface. It would also supply the sites of additional hydration and, by the concomitant swelling, the increased volume and radius of gyration measured. This increase in radius of gyration, it may be noted, is nearly the same as corresponding increases documented in other cases of cleft mechanisms, where clefts accommodate ligands of the same order of size [40,41,53,55].

Chemical modification studies [6,18] have demonstrated the involvement of tyrosine and tryptophan in the binding of riboflavin by RBP. Reorientation of these residues at low pH would lead to release of the vitamin by the carrier protein. A more disordered state for the residues associated with the near-UV region, that is, more freedom of rotation for the aromatic side chains [5], is in agreement with the observation that the increase in molecular volume in going from high to low pH outpaces the increase in hydration; it agrees also with the earlier mention of a reversal of net charge and of increased segmental motion. Increased exposure of aromatic groups in an opened-up aromatic-rich cleft would lead to less additional hydration than the increases in volume and surface would imply.

The observed changes in the molecular parameters of RBP indicate a fairly coherent description of the changes in structure that accompany the release of riboflavin at low pH. SAXS results document a change in tertiary structure at low pH characterized by an appreciable increase in volume with slightly decreased anisotropy. Analysis of the total surface data gives an estimate of the portion attributable to increased surface texture of the molecule. The change in radius of gyration is of the same order of magnitude as that associated with cleft closure in the case of several binding proteins reported in the literature. (It makes no essential difference that the mechanism in those cases was allosteric, whereas in the present case it is pH-induced.) The mechanism emerging from these observations had to be based on solution properties alone since, in contrast to proteins for which similar

mechanisms have been reported, no X-ray crystallographic data were available here. Subject to this reservation, a picture consistent with all observations is one in which the release of riboflavin by RBP involves the opening of a pre-existing aromatic-rich cleft in the protein molecule under conditions of low pH. In a similar situation, we have begun to use SAXS to study the deletion mutation of $\alpha_{s1}$-A casein (Farrell and Kumosinski, pages 61–71, in this issue) and its impact on casein functionality (Kumosinski, Pessen and Farrell, unpublished data, Abstract of the 7th International Scattering Conference, Prague, July 13–16, 1987).

In summary, then, SAXS is a technique that can be used to highlight both essential similarities and rather subtle differences in tertiary structure. It mirrors similarities between α-La and lysozyme that may be conjectured from the literature, but it also shows a sharp contrast between these proteins and ribonuclease, a protein of similar size but very different properties. SAXS further tracks the subtle changes in tertiary structure between the apo and holo forms of RBP, which correlate with the dramatic chemical changes attendant on its biological functioning. Since caseins and other food proteins have never been, and may never be, crystallized, SAXS studies in many cases will offer the only hope for investigating detailed molecular properties.

## REFERENCES


1 Aschaffenburg, R. and J. Drewry. 1957. Improved method for the preparation of crystalline β-lactoglobulin and α-lactalbumin from cow milk. Biochem. J. 65: 273–277.

2 Aune, K.C., 1968. Thermodynamics of the denaturation of lysozyme. Ph.D. Dissertation, Duke University, Durham, NC.

3 Becvar, J. and G. Palmer. 1982. The binding of flavin derivatives to the riboflavin-binding protein of egg white. J. Biol. Chem. 257: 5607–5617.

4 Beeman, W.W., P. Kaesberg, J.W. Anderegg and M.B. Webb. 1957. Sizes of particles and lattice defects. In: Handbuch der Physik (Flügge, S., ed.), p. 321–442, Springer, Berlin.

5 Beychok, S. 1966. Circular dichroism of biological macromolecules. Circular dichroism spectra of proteins and nucleic acids provide insights into solution conformations. Science 154: 1288–1299.

6 Blankenhorn, G. 1978. Riboflavin binding in egg-white flavoprotein: the role of tryptophan and tyrosine. Eur. J. Biochem. 82: 155–160.

7 Blankenhorn, G. 1980. Functional groups of egg-white flavoprotein involved in flavin binding. In: Flavins and Flavoproteins, Proceedings of the 6th International Symposium (Yagi, K. and Yamono, T., eds.), pp. 405–411, Japan Scientific Press, Tokyo.

8 Brew, K., T.C. Vanaman and R.L. Hill. 1967. Comparison of the amino acid sequence of bovine α-lactalbumin and hens egg white lysozyme. J. Biol. Chem. 242: 3747–3749.

9 Brown, E.M. and H.M. Farrell, Jr. 1978. Interaction of β-lactoglobulin and cytochrome c: complex formation and iron reduction. Arch. Biochem. Biophys. 185: 156–164.

10 Canfield, R.E. 1963. The amino acid sequence of egg white lysozyme. J. Biol. Chem. 238: 2698–2707.

11 Charlwood, P.A. 1957. Partial specific volumes of proteins in relation to composition and environment. J. Am. Chem. Soc. 79: 776–781.

12 Cowburn, D.A., E.M. Bradbury, C. Crane-Robinson and W.B. Gratzer. 1970. An investigation of the conformation of bovine α-lactalbumin by proton magnetic resonance and optical spectroscopy. Eur. J. Biochem. 14: 83–93.

13 Eaker, D.L. 1962. Structural and enzymatic studies with deslysyl forms of bovine pancreatic ribonuclease. Ph.D. Thesis, Rockerfeller Institute, New York.

14 Eigel, W.N., J.E. Butler, C.A. Ernstrom, H.M. Farrell, Jr., V.R. Harwalkar, R. Jenness and R. McL. Whitney. 1984. Nomenclature of proteins of cow's milk: fifth revision. J. Dairy Sci. 67: 1599–1631.

15 Fahey, P.F., D.W. Kupke and J.W. Beams. 1969. Effect of pressure on the apparent specific volume of proteins. Proc. Natl. Acad. Sci. USA 63: 548–555.

16 Farrell, H.M., Jr., M.J. Behe and J.A. Enyeart. 1987. Binding of p-nitrophenyl phosphate and other aromatic compounds by β-lactoglobulin. J. Dairy Sci. 70: 252–258.

17 Farrell, H.M., Jr., E.G. Buss and C.O. Claggett. 1970. The nature of the biochemical lesion in avian renal riboflavinuria. V. Elucidation of riboflavin transport in the laying hen. Int. J. Biochem. 1: 168–172.

18 Farrell, H.M., Jr., M.F. Malette, E.G. Buss and C.O. Claggett. 1969. The nature of the biochemical lesion in avian renal riboflavinuria. III. The isolation and characterization of the riboflavin-binding protein from egg albumen. Biochim. Biophys. Acta 194: 433–442.

19 Froehlich, J.A., A.H. Merill, Jr., C.O. Claggett and D.B. McCormick. 1980. Affinity chromatographic purification and comparison of riboflavin-binding proteins from laying hen liver and blood and from egg yolk. Comp. Biochem. Physiol. 66B: 397–401.

20 Georges, C., S. Guinand and J. Tonnelat. 1962. Etude thermodynamique de la dissociation réversible de la β-lactoglobuline B pour des pH supérieurs à 5,5. Biochim. Biophys. Acta 59: 737–739.

21 Godovac-Zimmermann, J., A. Conti, J. Liberatori and G.

Braunitzer. 1985. Homology between the primary structure of β-lactoglobulins and human retinol binding protein: evidence for a similar biological function? Biol. Chem. Hoppe-Seyler 366: 431–434.

22 Gordon, W.G., J.J. Basch and E.B. Kalan. 1961. Amino acid composition of β-lactoglobulins A, B, and AB. J. Biol. Chem. 236: 2908–2911.

23 Gordon, W.G. and J. Ziegler. 1955. Amino acid composition of crystalline α-lactalbumin. Arch. Biochem. Biophys. 57: 80–86.

24 Green, D.W., R. Aschaffenburg, A. Camerman, J.C. Coppola, P. Dunnill, R.M. Simmons, E.S. Komorowski, L. Sawyer, E.M.C. Turner and K.F. Woods. 1979. Structure of bovine β-lactoglobulin at 6Å resolution. J. Mol. Biol. 131: 375–397.

25 Guinier, A. 1939. La diffraction des rayons X aux très petits angles: application à l'étude de phénomènes ultramicroscopiques. An. Phys. (Paris) 12: 161–237.

26 Guinier, A. and G. Fournet. 1955. Small Angle Scattering of X-rays, pp. 24, 80, 133, Wiley, New York.

27 Kanarek, L. 1963. D.Sc. Thesis, Free University of Brussels, Brussels.

28 Kratky, O. 1963. X-ray small angle scattering with substances of biological interest in diluted solutions. In: Progress in Biophysics and Molecular Biology (Butler, J.A.V., H.E. Huxley and R.E. Zirkle, eds.), Vol. 13, pp. 105–173, Pergamon Press, MacMillan, New York.

29 Krigbaum, W.R. and F.R. Kügler. 1970. Molecular conformation of egg-white lysozyme and bovine α-lactalbumin in solution. Biochemistry 9: 1216–1223.

30 Kronman, M.J. 1968. Similarity in backbone conformation of egg white lysozyme and bovine α-lactalbumin. Biochem. Biophys. Res. Commun. 33: 535–541.

31 Kronman, M.J. and R.E. Andreotti. 1964. Inter- and intramolecular interactions of α-lactalbumin. I. The apparent heterogeneity at acid pH. Biochemistry 3: 1145–1151.

32 Kronman, M.J., S.K. Sinha and K. Brew. 1981. Characteristics of the binding of $Ca^{2+}$ and other divalent metal ions to bovine α-lactalbumin. J. Biol. Chem. 256: 8582–8587.

33 Kumosinski, T.F. and S.N. Timasheff. 1966. Molecular interactions in β-lactoglobulin. X. The stoichiometry of the β-lactoglobulin mixed tetramerization. J. Am. Chem. Soc. 88: 5635–5642.

34 Laemmli, U.K. 1970. Cleavage of structural proteins during the assembly of the head of bacteriophage T4. Nature (Lond.) 277: 680–685.

35 Lowry, O.H., N.J. Rosebrough, A.L. Farr and R.J. Randall. 1951. Protein measurement with the Folin phenol reagent. J. Biol. Chem. 193: 265–275.

36 Luzzati, V. 1957. Interprétation géométrique de la diffusion aux petits angles d'un faisceau de rayons X de section infiniment haute et étroite. Acta Crystallogr. 10: 136–138.

37 Luzzati, V. 1960. Interpretation des mesures absolues de diffusion centrale des rayons X en collimation ponctuelle ou linéaire: solutions des particules globulaire et de bâtonnets. Acta Crystallogr. 13: 939–945.

38 Luzzati, V., J. Witz and A. Nicolaieff. 1961. Determination of the mass and dimensions of proteins in solution by X-ray scattering measured on an absolute scale: example of lysozyme. J. Mol. Biol. 3: 367–378.

39 Luzzati, V., J. Witz and A. Nicolaieff. 1961. The structure of bovine serum albumin in solution at pH 5.3 and 3.6; study by absolute scattering of X-rays. J. Mol. Biol. 3: 379–392.

40 MacDonald, R.C., D.M. Engelman and T.A. Steitz. 1979. Small angle X-ray scattering of dimeric yeast hexokinase in solution. J. Biol. Chem. 254: 2942–2943.

41 MacDonald, R.C., T.A. Steitz and D.M. Engelman. 1979. Yeast hexokinase in solution exhibits a large conformational change upon binding glucose or glucose 6-phosphate. Biochemistry 18: 338–342.

42 Maw, A.J.G. 1954. Inherited riboflavin deficiency in chicken eggs. Poultry Sci. 33: 216–271.

43 McKenzie, H.A. and W.H. Sawyer. 1967. Effect of pH on β-lactoglobulins. Nature (Lond.) 214: 1101–1104.

44 Murakami, K., P.J. Andree and L.J. Berliner. 1982. Metal ion binding to α-lactalbumin species. Biochemistry 21: 5488–5494.

45 Nishikimi, M. and Y. Kyogoka. 1973. Flavin-protein interaction in egg white flavoprotein. J. Biochem. (Tokyo) 73: 1233–1242.

46 Osuga, D.T. and R.E. Feeney. 1968. Biochemistry of the egg-white proteins of the ratite group. Arch. Biochem. Biophys. 124: 560–574.

47 Pedersen, K.O. 1936. Ultracentrifugal and electrophoretic studies on the milk proteins. II. The lactoglobulin of Palmer. Biochem. J. 30: 961–970.

48 Permyakov, E.A., V.V. Yarmolenko, L.P. Kalinichenko, L.A. Morozova and E.A. Burstein. 1981. Calcium binding to α-lactalbumin: structural rearrangements and association constant by protein fluorescence changes. Biochem. Biophys. Res. Commun. 100: 191–197.

49 Pervaiz, S. and K. Brew. 1985. Homology of β-lactoglobulin, serum retinol binding protein, and protein HC. Science 228: 335–337.

50 Pessen, H., T.F. Kumosinski, S.N. Timasheff, R.R. Calhoun, Jr. and J.A. Connelly. 1970. A new absolute-scale small-angle X-ray scattering instrument. In: Advances in X-Ray Analysis (Henke, B.L., J.B. Newkirk and G.R. Mallett, eds.), Vol. 13, pp. 618–631, Plenum Press, New York.

51 Pessen, H., J.M. Purcell and H.M. Farrell, Jr. 1985. Proton relaxation rates of water in dilute solutions of β-lactoglobulin. Determination of cross relaxation and correlation with structural changes by the use of two genetic variants of a self-associating globular protein. Biochim. Biophys. Acta 228: 1–12.

52 Phillips, J.W. 1963. Physical and chemical properties of a riboflavin-binding protein. Ph.D. Thesis, Pennsylvania State University, University Park, PA.

53 Pickover, C.A., D.B. McKay, D.M. Engleman and T.A. Steitz. 1979. Substrate binding closes the cleft between the domains of yeast phosphoglycerate kinase. J. Biol. Chem. 254: 11323–11329.

54 Porod, G. 1951. The X-ray small-angle scattering of close-packed colloid system. Kolloid-Z. 124: 83–114.
55 Quiocho, F.A., G.L. Gilliland, M.E. Newcomer, D.M. Miller, III, J.W. Pflugrath, M.A. Saper and J.S. Olson. 1980. Structure and function of binding proteins for transport and chemotaxis in bacteria. Fed. Proc. Fed. Am. Soc. Exp. Biol. 39: 2103.
56 Roels, H., G. Préaux and R. Lontie. 1971. Polarimetric and chromatographic investigation of the irreversible transformation of β-lactoglobulin A and B upon alkaline denaturation. Biochimie 53: 1085–1093.
57 Rothen, A. 1940. Molecular weight and electrophoresis of crystalline ribonuclease. J. Gen. Physiol. 24: 203–211.
58 Shiga, K., K. Horiike, Y. Nishina, S. Otani, H. Watari and T. Yamano. 1979. A study of flavin-protein and flavoprotein-ligand interactions. Binding aspects and spectral properties of D-amino acid oxidase and riboflavin binding protein. J. Biochem. (Tokyo) 85: 931–941.
59 Smyth, D.G., W.H. Stein and S. Moore. 1963. The sequence of amino acid residues in bovine pancreatic ribonuclease: revisions and confirmations. J. Biol. Chem. 238: 227–234.
60 Soulé, J.L. 1957. La détermination des surfaces et des interfaces spécifiques par diffusion centrale du rayonnement X. I. Fondements théoriques. J. Phys. Radium Phys. Appl. Suppl. 18: 90A–102A.
61 Strosberg, A.D., C. Nihoul-Deconinck and L. Kanarek. 1970. Weak immunological cross-reaction between bovine α-lactalbumin and hen's egg-white lysozyme. Nature (Lond.) 227: 1241–1242.
62 Stuart, D.I., K.R. Acharya, N.P.C. Walker, S.G. Smith, M. Lewis and D.C. Phillips. 1986. α-lactalbumin possesses a novel calcium binding loop. Nature (Lond.) 324: 84–87.
63 Tanford, C., L.G. Bunville and Y. Nozaki. 1959. The reversible transformation of β-lactoglobulin at pH 7.5. J. Am. Chem. Soc. 81: 4032–4035.
64 Timasheff, S.N. 1963. The application of light scattering and small-angle X-ray scattering to interacting biological systems. In: Electromagnetic Scattering (Kerker, M., ed.), pp. 337–355, Pergamon, New York.
65 Timasheff, S.N. 1964. Light and small angle X-ray scattering and biological macromolecules. J. Chem. Ed. 41: 314–320.
66 Timasheff, S.N. 1964. The nature of interactions in proteins derived from milk. In: Symposium on Foods: Proteins and Their Reactions (Schultz, H.W. and A.F. Angelmeier, eds.), p. 174, Avi, Westport, CT.
67 Timasheff, S.N. and R. Townend. 1961. Molecular interactions in β-lactoglobulin. V. The association of the genetic species of β-lactoglobulin below the isoelectric point. J. Am. Chem. Soc. 83: 464–469.
68 Timasheff, S.N. and R. Townend. 1964. Structure of the β-lactoglobulin tetramer. Nature (Lond.) 203: 517–519.
69 Townend, R. 1965. β-lactoglobulins A and B: the environment of the Asp/Gly difference residue. Arch. Biochem. Biophys. 109: 1–6.
70 Townend, R., R.J. Winterbottom and S.N. Timasheff. 1960. Molecular interactions in β-lactoglobulin. II. Ultracentrifugal and electrophoretic studies of the association of β-lactoglobulin below its isoelectric point. J. Am. Chem. Soc. 82: 3161–3168.
71 Waissbluth, M.D. and R.A. Grieger. 1974. Alkaline denaturation of β-lactoglobulins. Activation parameters and effect on dye binding site. Biochemistry 13: 1285–1288.
72 Warme, D.K., F.A. Momay, S.V. Rumball, R.W. Tuttle and H.A. Scheraga. 1974. Computation of structures of homologous proteins. α-lactalbumin from lysozyme. Biochemistry 13: 768–782.
73 Winter, W.P., E.G. Buss, C.O. Claggett and R.V. Boucher. 1967. The nature of the biochemical lesion in avian renal riboflavinuria. II. The inherited change of a riboflavin-binding protein from blood and eggs. Comp. Biochem. Physiol. 22: 897–906.
74 Witz, J., S.N. Timasheff and V. Luzzati. 1964. Molecular interactions in β-lactoglobulin. VIII. Small-angle X-ray scattering investigation of the geometry of β-lactoglobulin A tetramerization. J. Am. Chem. Soc. 86: 168–173.